

CONSTITUTIVE EQUATION TO PREDICT THE FLOW STRESS AND THE PROCESSING MAPS OF THE Ni55Cr45 ALLOY

ŁUKASZEK-SOŁEK Aneta¹, CHYŁA Piotr^{2*}, ŚWIĄTONIOWSKI Andrzej², SZOSTAK Janusz²

¹AGH University of Science and Technology, Faculty of Metals Engineering and Industrial Computer Science, Cracow, Poland, EU

²AGH University of Science and Technology, Faculty of Mechanical Engineering and Robotics, Cracow, Poland, EU, * pchyla@agh.edu.pl

Abstract

The hot deformation behaviour of Ni55Cr45 alloy was investigated by isothermal compression test on the GLEEBLE 3800 thermo-mechanical simulator in the wide range of temperatures (750 - 1150 °C) and strain rates (1 - 100 s⁻¹). The experimental stress-strain data were employed to develop the constitutive equation and activation energy of the investigated Ni-Cr alloy. The correlation between the flow stress, temperature and strain rate at high temperatures was expressed by an Arrhenius type equation. The effects of temperature and strain rate on deformation behaviour were represented by Zener-Hollomon parameter in an exponent-type equation. Activation energy was calculated using a sine-hyperbolic type equation. The processing maps based on the Murty's approach were developed. The processing window and the flow instability areas were determined. Furthermore the experimental rolling test was conducted according to delineated processing parameters. The results of numerical simulation and experimental rolling test showed good agreement with the optimum hot deformation condition.

Keywords: Constitutive analysis, flow stress, activation energy, processing map

1. INTRODUCTION

The Dynamic Material Modelling (DMM) is based upon irreversible thermodynamics, and also upon continuum mechanics [1, 2]. Processing maps are an effective tool for optimizing materials workability. The processing maps show, in the process space contained in the function of temperature and log(strain rate), process conditions for the stable and unstable deformation, which means that they present "safe" and "unsafe" hot working conditions. The analysis of material flow during hot deformation made it possible to identify the most advantageous parameters in the processing windows [3 - 5]. Many scientists have been developing the processing maps in order to control and optimize the parameters of hot working processing for various kinds of metals and alloys [4 - 9]. The aim of present investigation was modeling the hot deformation behaviour of Ni55Cr45 alloy using constitutive equations and the processing map according Murty's approach. The most advantageous parameters of the metal forming process determined by processing windows were applied for the simulation and verification of the rolling process conducted on the Ni55Cr45 alloy. The conditions established during numerical modelling were also applied to the industrial rolling tests.

2. EXPERIMENTAL PROCEDURE

The material used in this investigation was the Ni55Cr45 alloy. The chemical composition (wt%) of the alloy in this study is as follows: 44.00 Cr, 1.00 Fe, 0.05 Mn, 0.003 Mo, 0.01 N, 0.115 Si and Ni balance. The cylindrical compression samples of 12 mm height and 10 mm diameter were prepared from the as-received cast bar. The isothermal compression tests were carried out using a Gleeble 3800 thermo-simulator with deformation temperature of 750 - 1150 °C and the strain rate of 1 - 100 s⁻¹. Based on the determined process parameters rolling technology was developed in the oval - oval - hexagonal system on a rolling mill with a cylinder diameter of 600 mm. It was assumed that the elongation factor (λ) in successive culverts would be about 1.1. In the first

instance segments with patterns were designed and then numerical calculations were made in the MES-based commercial program QForm. The most advantageous parameters of the rolling process determined by processing windows were applied for the simulation and verification of the rolling process in industrial conditions. For this purpose the forge rolling EUMUCO ECB 109 was used. The mill was installed at the workshop hall of tools factory „Kuźnia” S.A in Sułkowie. The rolling process was conducted in a machine group consisting of an electrical resistance furnace and also of a forge rolls. The following boundary conditions were assumed: workpiece temperature (1150 °C), tool temperature (20 °C), the time of workpiece transportation to the forge rolls (2 s), the time of workpiece cooling in a die cavity before rolling (1 s). The workpiece dimensions were 36 mm x 160 mm. The samples for metallographic tests were cut from obtained forgings after the forge rolling process.

3. RESULTS AND DISCUSSION

3.1. Constitutive equation

The constitutive equation for the describing of the deformation behaviour at elevated temperatures is generally expressed as follows [1, 2]:

$$\dot{\varepsilon} = A_i f(\sigma) \exp\left(-\frac{Q}{RT}\right) \quad (1)$$

where: $\dot{\varepsilon}$ - strain rate, Q - the deformation activation energy (kJ·mol⁻¹), R - the universal gas constant (8.314 J·mol⁻¹·K⁻¹), T - deformation temperature (K), A_i - material constant, and $f(\sigma)$ - the function of flow stress. The Zener-Hollomon parameter (so-called temperature-compensated strain rate) is calculated with the use of an exponent-type equation:

$$Z = \dot{\varepsilon} \exp\left(\frac{Q}{RT}\right) = A_i f(\sigma) \quad (2)$$

A relationship between the Zener-Hollomon parameter and flow stress [10 - 12] can be defined by the following constitutive equations:

$$Z = A_1 \cdot \sigma^{n_1} = 1.006 \cdot 10^{-21} \cdot \sigma^{21.76152}, \alpha\sigma < 0.8 \quad (3)$$

$$Z = A_2 \cdot \exp(\beta \cdot \sigma) = 1.15 \cdot 10^{15} \cdot \exp(0.04632 \cdot \sigma), \alpha\sigma > 1.2 \quad (4)$$

$$Z = A_3 \cdot [\sinh(\alpha \cdot \sigma)]^n = 5.95 \cdot 10^{25} \cdot [\sinh(0.002129 \cdot \sigma)]^{15.92568}, \text{for all } \sigma \quad (5)$$

where: $A_1, A_2, A_3, \alpha, \beta, n_1, n$ - materials' constant, and $\sigma = \sigma_i = \sigma_p$ - flow stress. Upon the basis of equations, the average values of the materials constants were determined from the $\ln \sigma, \sigma, \ln(\sinh(\alpha\sigma)) - \ln \dot{\varepsilon}$ relations (**Figure 1**) at constant true strain of 0.8:

$$n_1 = \left. \frac{\partial \ln \dot{\varepsilon}}{\partial \ln \sigma} \right|_T = 21.76152 \quad (6)$$

$$\beta = \left. \frac{\partial \ln \dot{\varepsilon}}{\partial \sigma} \right|_T = 0.04632 \quad (7)$$

$$n = \left. \frac{\partial \ln \dot{\varepsilon}}{\partial \ln \sinh(\alpha \cdot \sigma)} \right|_T = 15.92568 \quad (8)$$

$$\text{where: } \alpha = \frac{\beta}{n_1} = 0.002129 \quad (9)$$

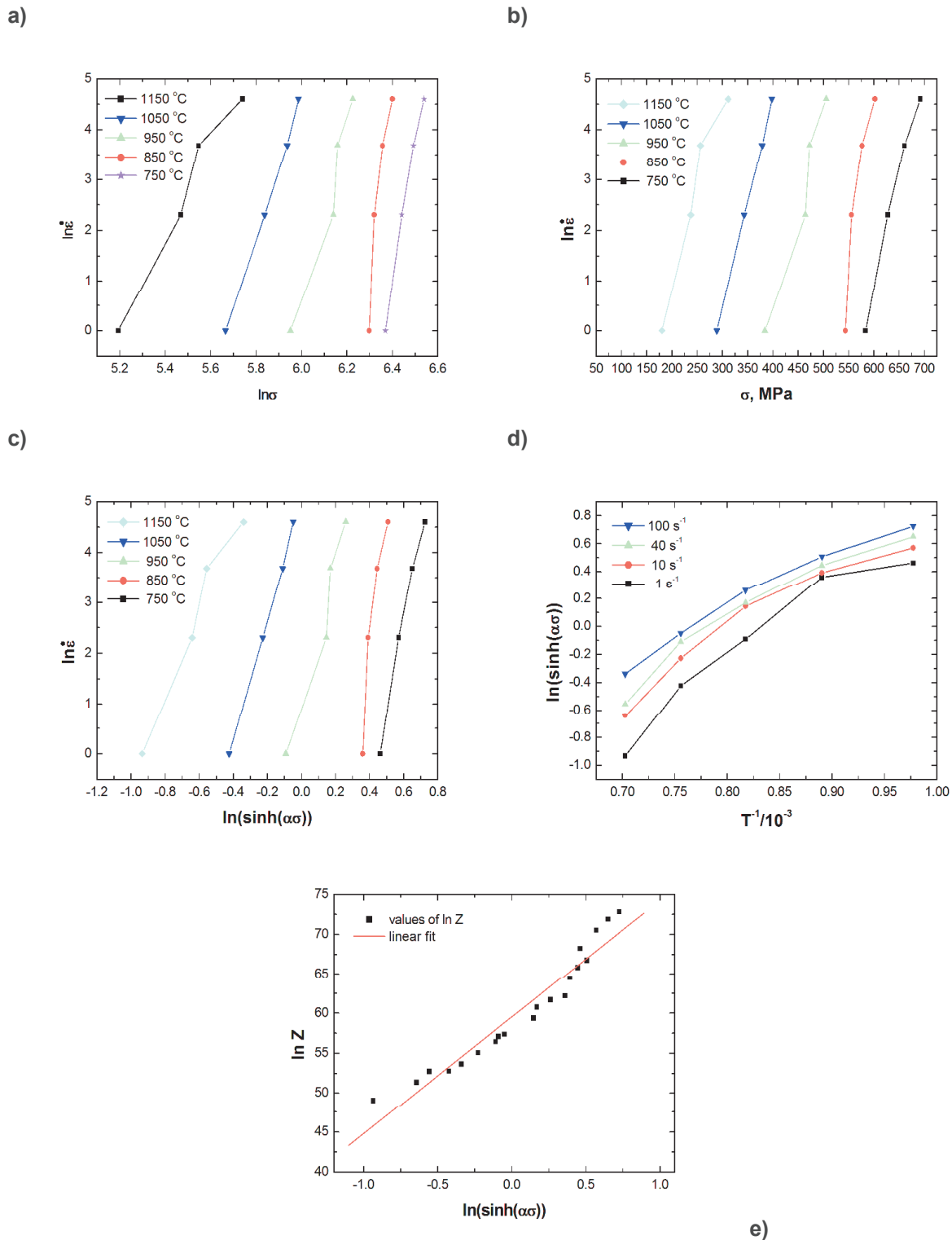


Figure 1 Relations between strain rate, flow stress, temperatures and parameter Z of Ni55Cr45: a) $\ln \sigma - \ln \dot{\epsilon}$, b) $\sigma - \ln \dot{\epsilon}$, c) $\ln(\sinh(\alpha\sigma)) - \ln \dot{\epsilon}$, d) $\ln(\sinh(\alpha\sigma)) - T^{-1}$, e) $\ln(\sinh(\alpha\sigma)) - \ln Z$

The peak stress of the studied Ni-Cr alloy maybe expressed as an equation [11, 12]

$$\sigma = \frac{1}{\alpha} \ln \left\{ \left(\frac{Z}{A} \right)^{\frac{1}{n}} + \left[\left(\frac{Z}{A} \right)^{\frac{2}{n}} + 1 \right]^{\frac{1}{2}} \right\} = \frac{1}{0.002129} \ln \left\{ \left(\frac{Z}{5.95 \cdot 10^{25}} \right)^{\frac{1}{15.92568}} + \left[\left(\frac{Z}{5.95 \cdot 10^{25}} \right)^{\frac{2}{15.92568}} + 1 \right]^{\frac{1}{2}} \right\} \quad (10)$$

where: parameter $Z = \dot{\epsilon} \cdot \exp\left(\frac{580122}{R \cdot T}\right)$. (11)

3.2. Activation energy

Activation energy for deformation Q provides valuable information about the fundamental deformation mechanism associated with microstructural evolution [11, 12]. The empirical value of activation energy Q can be expressed as:

$$Q = R \cdot n \cdot \left| \frac{\partial \ln(\sinh \alpha \cdot \sigma)}{\partial \left(\frac{1}{T}\right)} \right|_{\dot{\epsilon}} = 580.12 \frac{kJ}{mol} \quad (12)$$

For the Ni55Cr45 alloy, the hyperbolic sin law was found to be an appropriate relation, which resulted in the value of $580.12 \frac{kJ}{mol}$.

3.3. Processing maps

According to Murty's approach [6 - 9], the expression of power dissipation efficiency η is provided by:

$$\eta = \frac{J}{J_{max}} = 2 \left(1 - \frac{1}{\sigma \dot{\epsilon}} \int_0^{\dot{\epsilon}} \sigma d\dot{\epsilon} \right) \quad (13)$$

The instability parameter based upon Murty's criterion could be expressed as:

$$\xi = \frac{2m}{\eta} - 1 < 0 \quad (14)$$

The variation of the instability parameter with temperature and strain rate created the instability map, which can be superimposed on the power dissipation map to obtain the processing map [1].

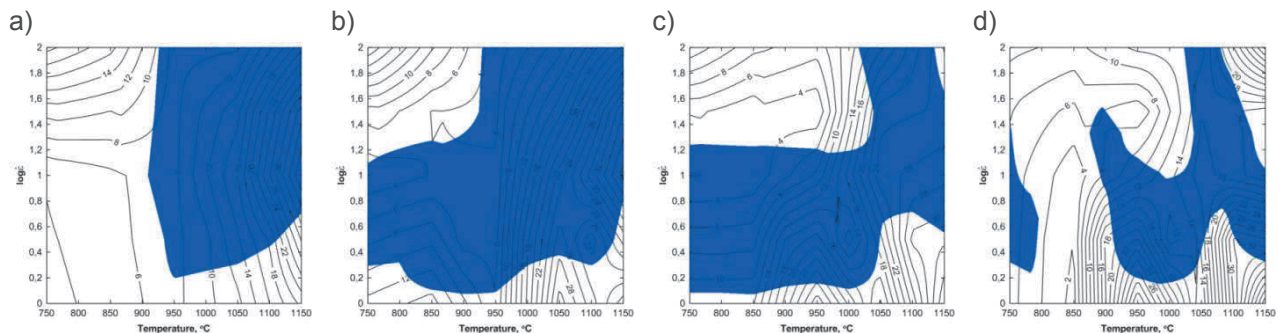


Figure 2 The processing maps of Ni55cr45 alloy at different true strain of: a) 0.2, b) 0.4, c) 0.6, d) 0.8. The shaded areas indicate the flow instability. Contour numbers represent percent efficiency of power dissipation.

The efficiency of power dissipation η and the instability parameter ξ is calculated for $\epsilon = 0.2, 0.4, 0.6, 0.8$ at different values of strain rate $\dot{\epsilon}$ and temperature T . **Figure 2** present the complex processing maps. For true strain of 0.8 (**Figure 2d**) in the processing map, three processing windows were differentiated and the two areas of instability. The preferred processing windows include significant parameters of the process. Processing window 1 is characterized by the following parameters: $\eta = 20 - 32\%$, $T = 910 - 1030 \text{ }^\circ\text{C}$, $\dot{\epsilon} = 1 - 1.6 \text{ s}^{-1}$. The next processing window presents the following parameters: $\eta = 20 - 46\%$, $T = 1070 - 1150 \text{ }^\circ\text{C}$, $\dot{\epsilon} = 1 - 2 \text{ s}^{-1}$. That window offers the high level of process efficiency. Processing window 3 includes parameters: $\eta = 20 - 34\%$, $T = 1080 - 1150 \text{ }^\circ\text{C}$, $\dot{\epsilon} = 45 - 100 \text{ s}^{-1}$. The area of instability of material flow I is situated at the temperature of $750 - 800 \text{ }^\circ\text{C}$ for strain rate $1.8 - 25 \text{ s}^{-1}$. Area instability II includes an extensive surface of non-

asymmetrical shape and the following parameters: $T = 860 - 1150 \text{ }^\circ\text{C}$, $\dot{\epsilon} = 1.6 - 100 \text{ s}^{-1}$. The maps presented in **Figures 2a, b, c** for true strain of 0.6, 0.4 and 0.2 differ one from another in terms of the size of the „safe“ and „unsafe“ areas. Processing windows: 1, 2 for $\epsilon = 0.6$ undergo the substantial differentiation of the significant parameters of the process, which means: $\eta_1 = 20 - 30\%$, $T_1 = 900 - 1010 \text{ }^\circ\text{C}$, $\dot{\epsilon}_1 = 1 - 1.3 \text{ s}^{-1}$, $\eta_2 = 20 - 34\%$, $T_2 = 1070 - 1150 \text{ }^\circ\text{C}$, $\dot{\epsilon}_2 = 1 - 3.1 \text{ s}^{-1}$. The processing window 3 was eliminated as a result of increase in the instability area. In the case of true strain of 0.4, on the processing maps was differentiated only one processing window, having the following parameters: $\eta_1 = 20 - 30\%$, $T_1 = 1025 - 1150 \text{ }^\circ\text{C}$, $\dot{\epsilon}_1 = 1 - 2 \text{ s}^{-1}$. On the processing map for intermediary true strain of 0.2, we distinguish one processing window. The window underwent decrease and having the following parameters: $\eta_1 = 18 - 30\%$, $T_1 = 1125 - 1150 \text{ }^\circ\text{C}$, $\dot{\epsilon}_1 = 1 - 4 \text{ s}^{-1}$. On the processing map for the true strain of 0.6, 0.4 and 0.2 (**Figures 2a, b and c**), there remain one area of instability formed from the combination of the two occurring in the case of the true strain of 0.8. The instability areas ought to be avoided whilst conducting the metal forming processes.

3.4. Validation of processing maps

In **Figure 3**, the results of numerical simulation and also of rolling in industrial condition were presented.

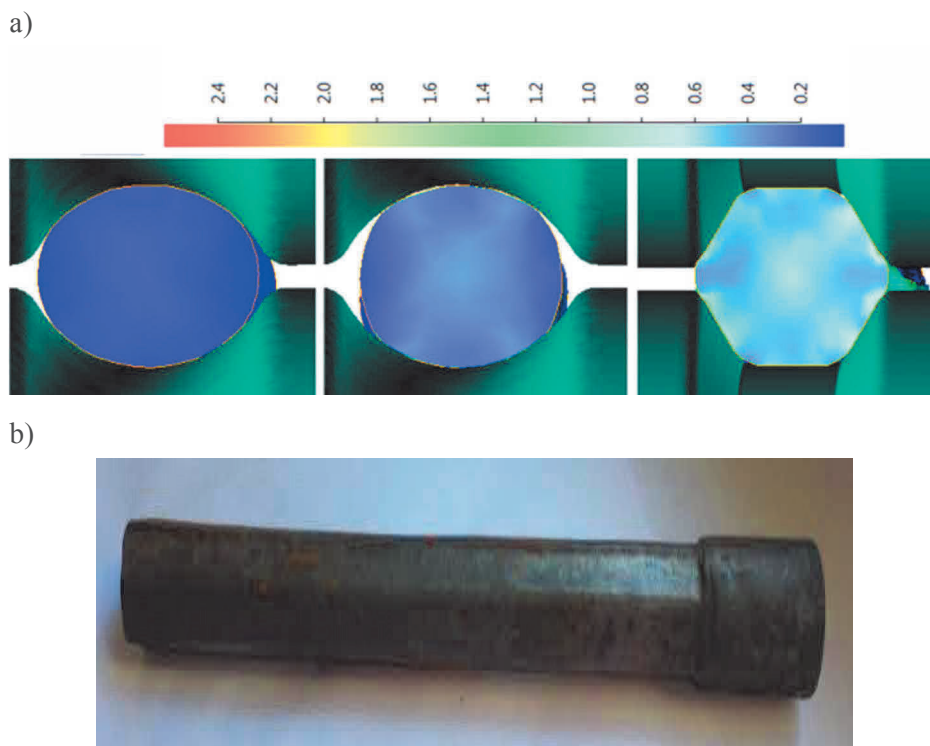


Figure 3 The results of forged bars in the oval - oval - hexagonal system: a) the numerical simulation, b) the industrial forge rolling process (The workpiece after the initial heat treatment.)

Measurements of the hexagonal bars revealed that their geometrical dimensions remained consistent with the results of the computer simulation and that the maximum deviation from the assumed linear dimensions was in the range $2.7 \div 6.1\%$. The **Figure 4** shows the microstructure of the forgings material (hexagonal rod) immediately after the deformation process.

The large dispersions likely to be carbonitrides or dispersions from the technological process were observed in the microstructure. The alloy matrix was $\gamma (\text{Ni}_{1-y}\text{Cr}_y)$.

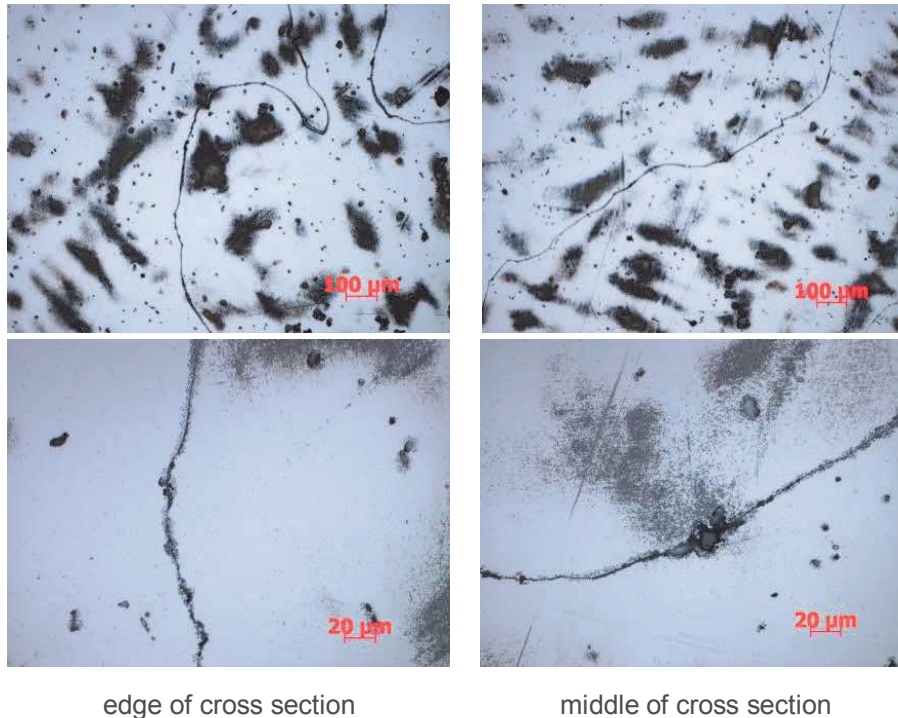


Figure 4 Microstructure of the Ni55Cr45 alloy (hexagonal bar) after the forge rolling process [13]

4. CONCLUSION

The hot deformation behaviour of Ni55Cr45 alloy was studied through constitutive analysis considering the effect of deformation parameters. Isothermal compression test were conducted on Gleeble 3800 thermomechanical simulator to predict the hot deformation behaviour. The relation between stress and Zener-Hollomon parameter was analyzed via the hyperbolic sine function. Therefore, the value of activation energy and the materials constants were determined. The processing maps were constructed by superimposition of the power dissipation and the instability maps. The appropriate processing parameters for hot deformation were established. The processing window 2 was successfully applied in the rolling process.

ACKNOWLEDGEMENTS

The research project was financed by the Ministry of Science and Higher Education (AGH-UST statutory research project no. 11.11.130.957)

REFERENCES

- [1] PRASAD, Y.V.R.K, SASIDHARA, S. (ed.) *Hot working guide: A compendium of processing maps*. ASM International, 1997.
- [2] DIETER, G.E., KUHN, H.A., SEMIATIN, S.L. *Handbook of Workability and Process Design*. ASM International, 2003.
- [3] LIU, J., CUI, Z., LI, C. Analysis of metal workability by integration of FEM and 3-D processing maps. *Journal of Materials Processing Technology*, 2008, vol. 205, pp.497-505.
- [4] WANG, J., DONG, J., ZHANG, M., XIE, X. Hot working characteristics of nickel-base superalloy 740H during compression. *Materials Science and Engineering A*, 2013, vol. 566, pp. 61-70.
- [5] WEN, D.X., LIN, Y.C., LI, H.B., CHEN, X.M., DENG, J., LI, L.T. Hot deformation and processing map of a typical Ni-based superalloy. *Materials Science and Engineering A*, 2014, vol. 591, pp.183-192.

- [6] MURTY, N.S.V.S., RAO, N.B. On the development of instability criteria during hot working with reference to IN 718. *Materials Science and Engineering A*, 1998, vol. 254, pp.76-82.
- [7] MURTY, N.S.V.S., RAO, N.B., KASHYAP, B.P. Identification of flow instabilities in the processing maps of AISI 304 stainless steel. *Journal of Materials Processing Technology*, 2005, vol. 166, pp.268-278.
- [8] MURTY, S.V.S.N., RAO, B.N. *On the flow localization concepts in the processing maps of IN718. Materials Science and Engineering A*, 1999, vol. 267, pp.159-161.
- [9] MURTY, N.S.V.S., RAO, N.B., KASHYAP, B.P. Instability criteria for hot deformation of materials. *International Materials Reviews*, 2000, vol. 45, pp. 15-26.
- [10] MURTY, N.S.V.S., SARMA, M.S., RAO, N.B. On the evaluation of efficiency parameters in processing maps. *Metallurgical and Materials Transactions A*, 1997, vol. 28A, pp.1581-1582.
- [11] HAJARI, A., MORAKABATI, M., ABBASI S, A., BADRI, H. Constitutive modeling for high-temperature flow behavior of Ti-6242S alloy. *Materials Science & Engineering A*, 2017, vol. 681, pp.103-113.
- [12] ZHANG, Y., JIANG, S., ZHAO, Y., LIU, S. Constitutive equation and processing map of equiatomic NiTi shape memory alloy under hot plastic deformation. *Trans. Nonferrous Met. Soc. China*, 2016, vol. 26 pp. 2152–2161.
- [13] ŚWIĄTONIOWSKI, A. (ed.) *Modyfikacja nadstopów o kompozycji na bazie niklu i chromu poprzez odkształcenie w procesie walcowania*. Akademia Górniczo-Hutnicza im. Stanisława Staszica w Cracowie. Wydział Inżynierii Mechanicznej i Robotyki, 2013.